Multimodality Imaging of Sinus Venosus Atrial Septal Defect: A Challenging Diagnosis in Adults

Jessica K. Qiu, MD, Daniel Bamira, MD, Alan F. Vainrib, MD, Larry A. Latson, MD, Dan G. Halpern, MD, Anne Chun, MD, and Muhamed Saric, MD, PhD, *New York, New York*

INTRODUCTION

Congenital heart disease is the most common congenital birth defect, affecting approximately nine per 1,000 live births.[1] Atrial septal defects (ASDs) are among the most prevalent forms of congenital heart disease, comprising roughly 10% of cases.[1] Of the several types of ASDs, secundum ASDs (75%) and primum ASDs (15%) occur most frequently. Sinus venosus ASD (SVASD) is a rare variant, accounting for 5%-10% of all ASDs.[2]

Sinus venosus ASD was first described in 1858 and first named as such in a 1956 report.[3,4] The characteristic defect of SVASD is the abnormal insertion of the superior vena cava (SVC) or inferior vena cava (IVC), which overrides the interatrial septum. The SVC-type SVASD (also referred to as superior ASD) occurs more often than the IVC-type SVASD (also referred to as inferior ASD).[5] Partial anomalous pulmonary venous return (PAPVR) is a frequently associated condition.

Echocardiography is the primary diagnostic modality of SVASD, although cardiac computed tomography (CCT), cardiovascular magnetic resonance (CMR), and cardiac catheterization are also utilized for further diagnostic clarification and management planning. Here we describe four adult cases of SVASD with a special focus on the incremental value of various imaging modalities used during the workup of this uncommon condition.

CASE PRESENTATIONS

Case 1

A previously healthy 25-year-old man presented with intermittent chest pain, dyspnea, and palpitations. An electrocardiogram (ECG) showed sinus rhythm with incomplete right bundle branch block. A transthoracic echocardiogram (TTE) revealed severe right heart dilatation (basal right ventricular [RV] linear dimension in apical four-chamber view of 4.7 cm; upper limit of normal of 4.1 cm).[6] There was interventricular septal motion indicative of RV volume overload, no significant tricuspid or pulmonic regurgitation, and no obvious intracardiac shunt on color Doppler (Video 1). The ratio of pulmonary to systemic blood flow (Qp:Qs) was roughly 3:1 by quantitative Doppler (Figure 1). Right ventricular systolic function was preserved (tricuspid annular plane systolic excursion, 3.5 cm; lower limit of normal, 1.7 cm).

Subsequent transesophageal echocardiography (TEE) revealed a large SVC-type SVASD (24 mm × 33 mm) with a left-to-right shunt and anomalous drainage of the right upper and middle pulmonary veins into the SVC (Figure 2, Videos 2 and 3). A small patent foramen ovale (PFO) was also noted that caused additional left-to-right shunt.

Three weeks later, he underwent successful surgical repair with an autologous pericardial patch sewn in the SVC, baffling the pulmonary venous return through the SVASD into the left atrium. The PFO was closed primarily.

A TTE obtained 4 months following the repair demonstrated interval improvement of the right heart dilatation. The RV size had normalized 1 year later (basal RV linear dimension, 3.8 cm), and RV systolic function remained normal (tricuspid annular plane systolic excursion, 1.9 cm). He continues to do well since his surgery.

Case 2

A 35-year-old man with no significant medical history presented with a complaint of persistent cough refractory to treatment with azithromycin, albuterol, and cough suppressants. His chest X-ray demonstrated an enlarged cardiac silhouette without pulmonary pathology. An ECG showed sinus rhythm with incomplete right bundle branch block. After a cardiac murmur was noted on exam, he was referred for TTE.

Transthoracic echocardiogram revealed a dilated RV (basal RV linear dimension, 5.1 cm) and prominent inflow from the SVC into the right atrium seen on color Doppler in subcostal views raising the possibility of an SVASD. Right ventricular systolic function was diminished (tricuspid annular tissue Doppler systolic [S'] peak velocity, 8 cm/sec; normal > 9.5 cm/sec).

Subsequent three-dimensional (3D) TEE confirmed the diagnosis of a large SVC-type SVASD measuring 1.95 cm × 1.81 cm (area = 2.8 cm^2) with left-to-right shunt as well as a PFO. Nongated contrast-enhanced CCT (Figure 3) showed both the SVASD and the PAPVR of the right upper and middle pulmonary veins into the SVC.

He underwent successful surgical repair with an autologous pericardial patch sewn in the SVC, baffling the pulmonary venous return through the SVASD into the left atrium, as well as primary closure of his PFO. Postrepair he leads an active lifestyle with regular running and cycling. Repeat TTE 2 years later revealed interval resolution of RV dilatation (basal RV linear dimension, 4.0 cm).

Case 3

A 53-year-old woman with a history of hypertension and anxiety was referred to cardiology for evaluation of tachycardia and dyspnea on exertion. Transthoracic echocardiogram showed severe RV dilatation

From the Leon H. Charney Division of Cardiology (J.K.Q., D.B., A.F.V., D.G.H., M.S.), Department of Radiology (L.A.L.), and Department of Pediatrics (A.C.), NYU Grossman School of Medicine, NYU Langone Health, New York, New York.

Keywords: Atrial septal defect, Sinus venosus, 3D echocardiography, Magnetic resonance imaging, Computed tomography

Conflicts of Interest: None.

Correspondence: Muhamed Saric, MD, PhD, Adult Echocardiography Laboratory, 550 First Avenue, New York, NY 10016 (E-mail: *Muhamed.Saric@nyulangone.org*).

2468-6441

https://doi.org/10.1016/j.case.2021.12.002

VIDEO HIGHLIGHTS

Video 1: Case 1: SVC-type SVASD on TTE in adult. Transthoracic echocardiographic clip demonstrating severe right heart dilatation and RV overload without significant valvular pathology or obvious intracardiac shunt. *LA*, Left atrium; *LV*, left ventricle; *RA*, right atrium.

Video 2: Case 1: SVC-type SVASD on 2D TEE in adult. Two-dimensional TEE clip demonstrating direct visualization of a large SVC-type SVASD. *Ao*, Aorta; *LA*, left atrium; *RA*, right atrium; *RUPV*, right upper pulmonary vein.

Video 3: Case 1: SVC-type SVASD on 3D TEE in adult. Three-dimensional TEE clip showing a large SVC-type SVASD from the right atrial perspective. *RA*, Right atrium.

Video 4: Case 4: IVC-type SVASD in adult on TTE and TEE. Transthoracic echocardiography and 2D TTE clips demonstrating an IVC-type SVASD and associated overriding IVC. *LA*, Left atrium; *RA*, right atrium.

Video 5: An SVC-type SVASD with anomalous pulmonary venous drainage on TTE in a child. Pediatric TTE showing SVC-type SVASD with anomalous pulmonary venous drainage from the subcostal view. *LA*, Left atrium; *RA*, right atrium.

Video 6: An IVC-type SVASD with anomalous pulmonary venous drainage on TTE in a child. Pediatric TTE showing IVC-type SVASD with anomalous pulmonary venous drainage. *LA*, Left atrium; *RA*, right atrium.

View the video content online at www.cvcasejournal.com.

and elevated velocities across the pulmonic valve (Vmax = 2.6 m/sec), suggestive of possible pulmonic stenosis or shunt and no other obvious abnormality.

Cardiovascular magnetic resonance (CMR) revealed a large 2.1 cm SVC-type SVASD with a large left-to-right shunt and calculated Qp:Qs of 3:1 (Figure 4). It also demonstrated anomalous connection of the right upper pulmonary veins to the SVC and drainage of the right middle pulmonary vein into the atria straddling the ASD. The right ventricle was moderately dilated (indexed volume, 135 mL/m^2) with normal systolic function (RV ejection fraction = 60%).

Cardiac catheterization revealed oxygen saturation step-up in the main pulmonary artery (94%), a Qp:Qs >3:1, normal pulmonary artery pressures and pulmonary vascular resistance, and angiographically normal coronary arteries.

Three months later, she underwent successful surgical repair with an autologous pericardial patch sewn in the SVC, baffling the pulmonary venous return through the SVASD into the left atrium. A PFO was noted intraoperatively and was closed primarily. Following the repair, she has been doing well, with improvement in right heart size on subsequent TTE.

Case 4

A 28-year-old man presented with chronic progressive chest pressure, dyspnea on exertion, and decreased exercise tolerance. Transthoracic and transesophageal echocardiograms demonstrated an aneurysmal atrial septum with an inferior septal defect measuring 1.8 cm and a dilated IVC overriding the defect (Figure 5A and B, Video 4). An anomalous right lower pulmonary vein draining into the right atrium adjacent to the defect was also visualized.

Subsequent CMR confirmed the PAPVR of the right lower pulmonary vein at the confluence of the right atrium and IVC overriding an IVC-type SVASD (Figure 5C and D). There was a large left-to-right shunt with calculated Qp:Qs of 3:1, as well as severe right heart and pulmonary artery dilation.

He underwent successful surgical repair with an autologous pericardial patch sewn in the IVC, baffling the pulmonary venous return through the SVASD into the left atrium. No residual defect or shunt was appreciated on subsequent TTE. He now enjoys a physically active lifestyle.

DISCUSSION

Sinus venosus ASD is caused by abnormal incorporation of the right horn of the sinus venosus into the right atrium during normal

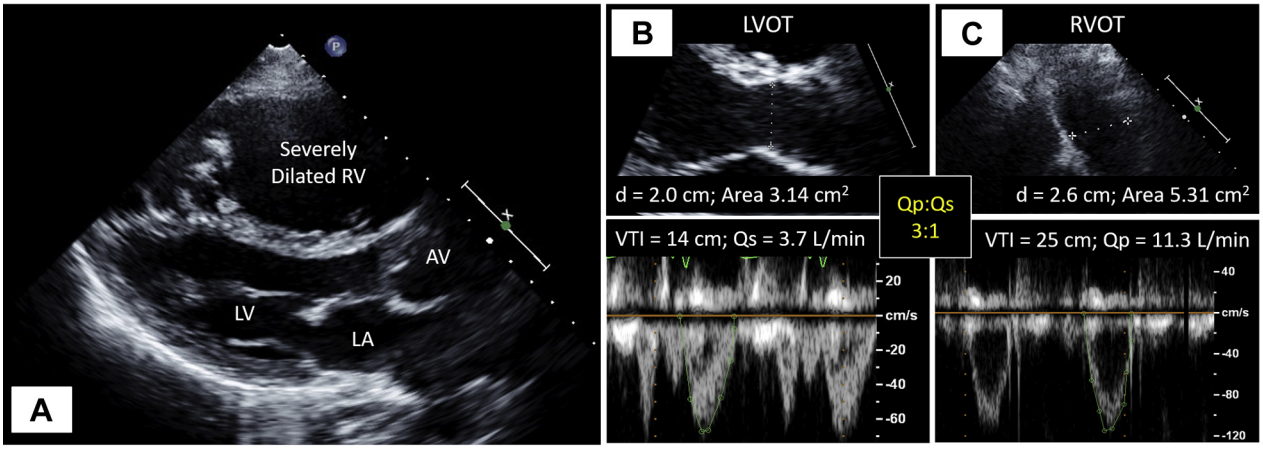

Figure 1 Case 1: SVC-type SVASD on TTE in adult. Direct demonstration of the actual SVC-type SVASD is often difficult on TTE in adults. Such a diagnosis should be suspected when there is an unexplained right heart dilatation **(A)** and when Doppler imaging demonstrates a significant left-to-right shunt **(B and C)**. Video 1 demonstrates significant and unexplained right heart dilatation. *AV*, Aortic valve; *d*, diameter; *LA*, left atrium; *LV*, left ventricle; *LVOT*, left ventricular outflow tract; *Qp*, pulmonic flow; *Qs*, systemic flow; *RVOT*, RV outflow tracts; *VTI*, velocity-time integral.

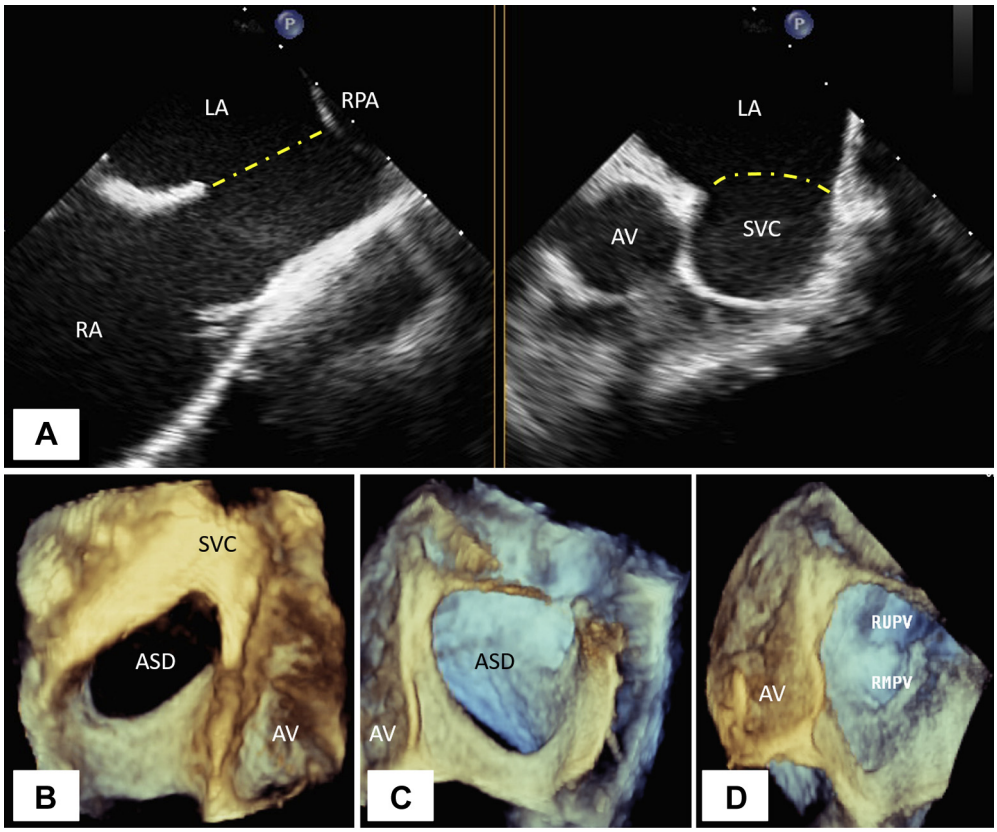

Figure 2 Case 1: SVC-type SVASD with anomalous pulmonary venous drainage on TEE in adult. An SVC-type SVASD can be directly demonstrated on 2D TEE **(A)** and 3D TEE **(B, C, and D)**. Video 2 corresponds to panel A. Video 3 corresponds to panels B and C. To successfully image this type of ASD on TEE, it is important to visualize the SVC in short- and long-axis views on 2D TEE first, followed by 3D zoom imaging of the defect. The 3D data set is then rotated using the TUPLE maneuver previously published by our group.[7] *AV*, Aortic valve; *LA*, left atrium; *RA*, right atrium; *RMPV*, right middle pulmonary vein; *RPA*, right pulmonary artery; *RUPV*, right upper pulmonary vein.

embryonic development, resulting in abnormal insertion of the caval veins.[8] There is an almost equal prevalence of SVASD between male and female patients; this is in contrast to the more common secundum ASD in which female patients significantly outnumber male patients.[5] Sinus venosus ASD is frequently associated with anomalous drainage of the right upper and middle pulmonary veins. Scimitar syndrome, another rare congenital heart defect, is similarly characterized by anomalous pulmonary venous drainage to the IVC, but notably the caval veins are inserted normally and no ASD is formed.[9] The physiologic consequence of the defect in SVASD is an often very large left-to-right shunt due to a combination of the ASD itself and PAPVR. Patients with long-standing uncorrected shunts may develop pulmonary hypertension and, in severe cases, Eisenmenger syndrome.[5]

Even with a large or hemodynamically significant shunt, patients may not present until the second or third decade of life. Symptoms on presentation commonly include fatigue, dyspnea, exercise intolerance, and palpitations. Patients with SVASD are at risk of developing atrial arrhythmias, particularly atrial fibrillation and atrial flutter.[2] The proximity of the defect to the sinus node also predisposes patients with SVC-type sinus venosus to sinus node dysfunction.[2]

In adults, SVASD can be challenging to diagnose accurately, especially by TTE. Our case series demonstrates the importance of multimodality imaging in diagnosing SVASD; TTE, TEE, CCT, CMR, and cardiac catheterization each confer incremental value for the anatomic and hemodynamic assessment of this rare condition.

Right heart dilatation can be caused by several conditions, including ASD, SVASD, coronary sinus defect, PAPVR, tricuspid or pulmonary valvular dysfunction, severe RV outflow tract obstruction, pulmonary hypertension, acute pulmonary embolism, and myocardial disease. Typically, SVASD is suspected on TTE when there is marked RV dilatation due to RV volume overload without an obvious etiology such as significant tricuspid or pulmonic regurgitation.[10] Additionally, detection of a PFO in a patient with unexplained, disproportionate RV dilatation should also raise concern for the presence of a coronary sinus defect or SVASD. While the septal defect of SVASD is usually difficult to visualize on standard TTE views in adults, it is often possible to view on pediatric TTE (Figures 6 and 7, Videos 5 and 6). In a review of 154 pediatric and adult patients with a known ASD, the sensitivity of TTE was 100% for diagnosing secundum ASD and 89% for primum ASD, whereas it was only 44% for SVASD.[11] The sensitivity is even lower in adults due to poorer acoustic windows and the posterior location of the defect.[5,10]

The parasternal short-axis view may be particularly useful for identifying possible SVASD in pediatric patients, as well as the subcostal parasagittal and right parasternal views in both pediatric and adult patients.[10,12,13] Moreover, in SVC-type ASD, a superiorly angled

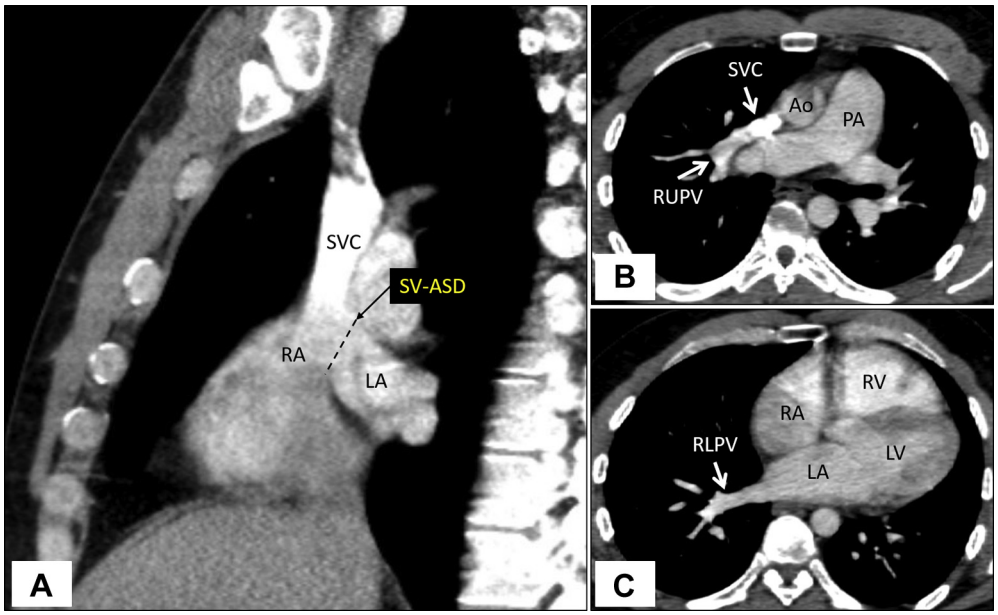

Figure 3 Case 2: SVC-type SVASD with anomalous pulmonary venous drainage on CCT in adult. **(A)** Sagittal view demonstrates abnormal interatrial communication indicative of an SVC-type SVASD. **(B)** The RUPV drains anomalously into the SVC as visualized on an axial cut. **(C)** In contrast, the RLPV drains normally into the left atrium on an axial cut. *Ao*, Ascending aorta; *LA*, left atrium; *LV*, left ventricle; *PA*, main pulmonary artery; *RA*, right atrium; *RLPV*, right lower pulmonary vein; *RUPV*, right upper pulmonary vein.

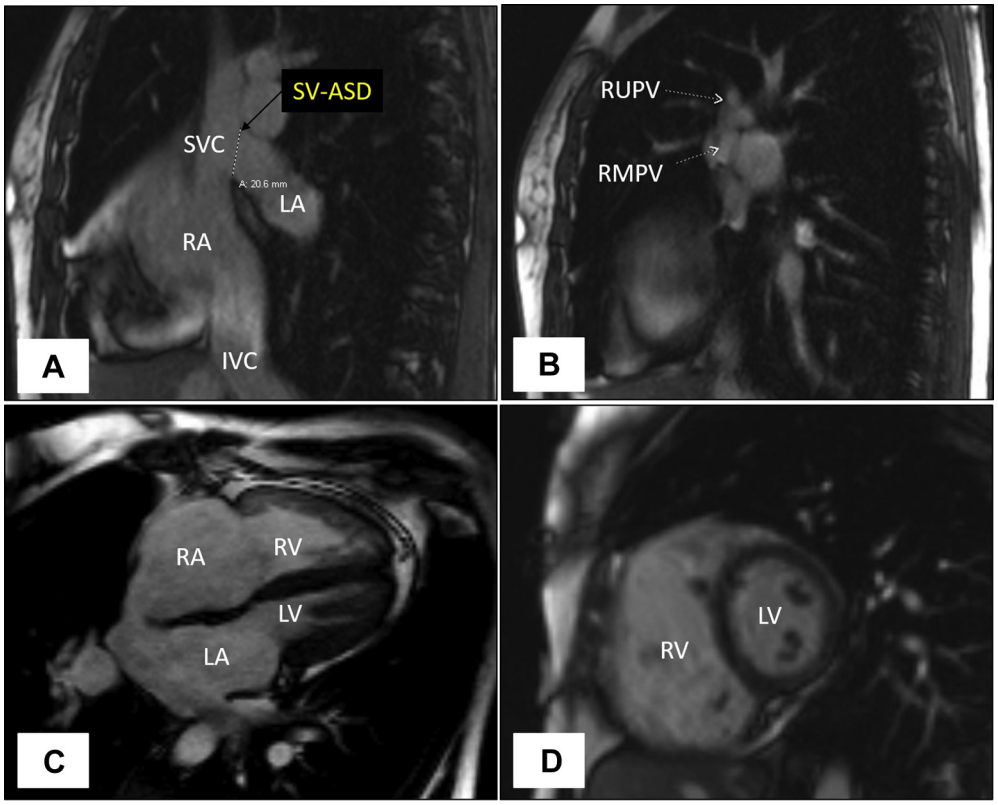

Figure 4 Case 3: SVC-type SVASD with anomalous pulmonary venous drainage on CMR in adult. Sagittal cuts demonstrated an SVC-type SVASD **(A)** and anomalous pulmonary venous drainage **(B)**. Note the right heart dilatation in panels **C** and **D** resulting from a double shunt (from ASD and anomalous pulmonary venous drainage). *LA*, Left atrium; *LV*, left ventricle; *RA*, right atrium; *RMPV*, right middle pulmonary vein; *RUPV*, right upper pulmonary vein.

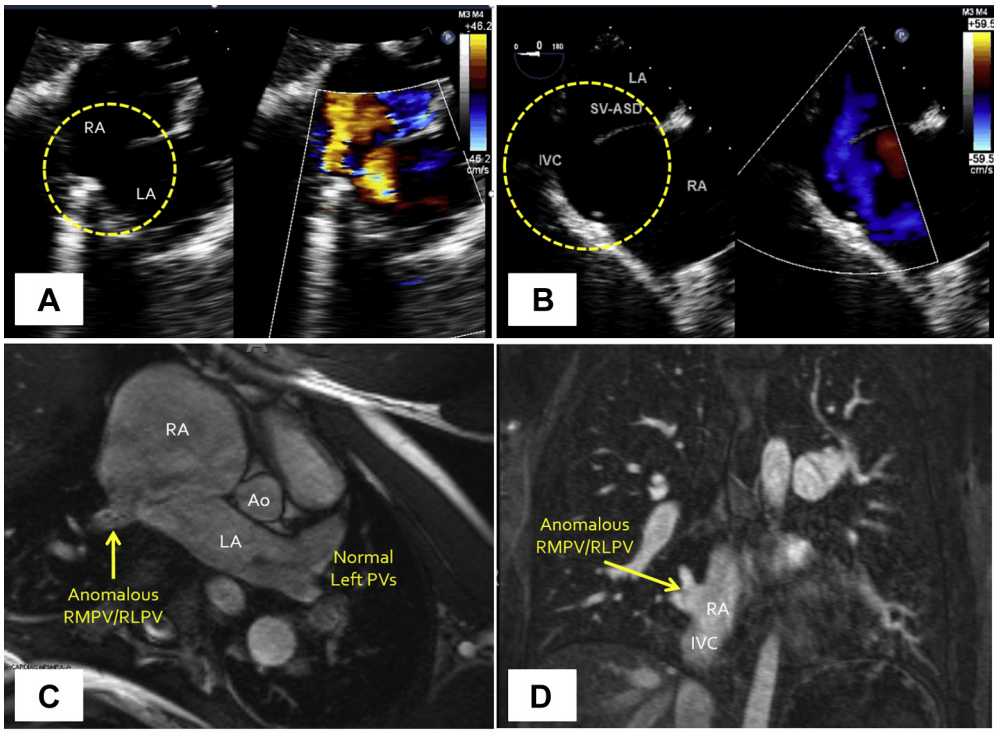

Figure 5 Case 4: IVC-type SVASD in adult on TTE, TEE, and CMR. Inferoposteriorly located IVC-type SVC is visualized on subcostal TTE view **(A)** and 2D TEE **(B)** with and without color Doppler. Cardiovascular magnetic resonance demonstrates anomalous pulmonary venous drainage **(C and D)**. Video 4 corresponds to panels A and B. *Ao*, Ascending aorta; *LA*, left atrium; *PVs*, pulmonary veins; *RLPV*, right lower pulmonary vein; *RMPV*, right middle pulmonary vein.

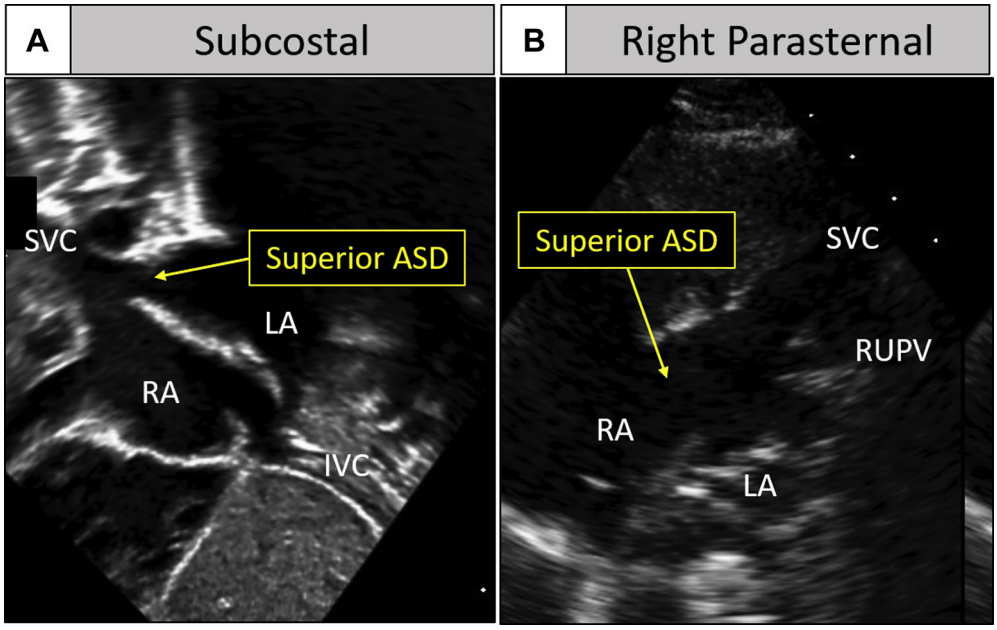

Figure 6 An SVC-type SVASD with anomalous pulmonary venous drainage on TTE in a child, as visualized by subcostal **(A)** and right parasternal **(B)** views. On pediatric TTE, it is often easier to demonstrate the SVC-type SVASD (also referred to as superior ASD) and associated anomalous pulmonary venous drainage than in adults. Video 5 corresponds to this figure. *LA*, Left atrium; *RA*, right atrium; *RUPV*, right upper pulmonary vein.

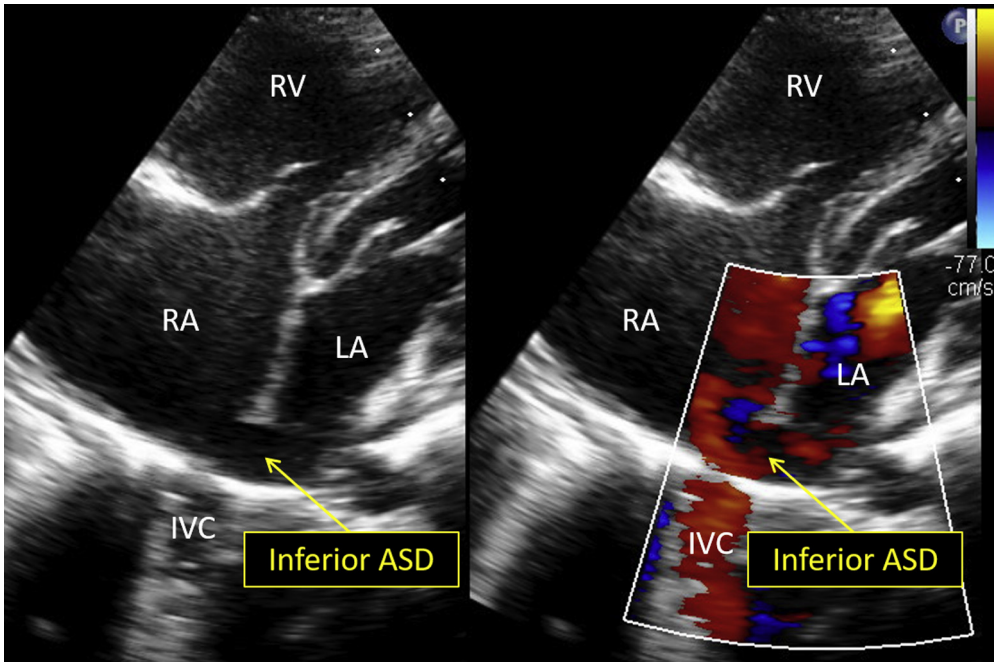

Figure 7 An IVC-type SVASD with anomalous pulmonary venous drainage on TTE in a child. On pediatric TTE, it is often easier to demonstrate the IVC-type SVASD (also referred to as inferior ASD) with an overriding IVC than in adults. Video 6 corresponds to this figure. *LA*, Left atrium; *RA*, right atrium.

subcostal view may allow the echocardiographer to visualize not only the SVASD but also the right superior anomalous venous return.

Contrast echocardiography with intravenous agitated saline may enhance the sensitivity of TTE in diagnosing SVASD via visualization of the bubbles traveling across the defect. In cases of superior SVASD with an overriding SVC, bubbles can appear nearly simultaneously in both atria due to a small amount of right-to-left shunting, although the predominant hemodynamic consequence of the defect is left-to-right shunting.[14] Agitated saline "bubble" studies are also useful for confirming absence of baffle leak following surgical repair.

Transesophageal echocardiography is indicated in all cases of suspected congenital heart disease with nondiagnostic or inadequate TTE images.[15] Transesophageal echocardiography has been shown to detect up to 20% of SVASDs that were initially missed on TTE.[10] Additionally, TEE is superior at consistently demonstrating anomalous pulmonary venous return.[10,16]

Three-dimensional echocardiography confers several advantages compared with conventional two-dimensional (2D) echocardiography in congenital heart disease, although it requires additional training and skill. The realistic images generated by 3D echocardiography more easily facilitate correct spatial orientation and understanding of complex cardiac anatomy. Three-dimensional echocardiography also provides more accurate cardiac chamber volumes, including RV volume, as it relies on voxel count per unit volume rather the geometric assumptions of 2D echocardiography.[17]

Cardiac computed tomography and CMR allow for noninvasive examination of the interatrial septum and delineation of the pulmonary venous anatomy.[18] Electrocardiogram gating of CCT enables the measurement of RV volumes as in CMR. Traditionally, the lack of ionizing radiation used in CMR was thought to be preferred in pediatric cases for which the precise anatomy remains unclear even after TTE and TEE.[19,20] However, the current ability to acquire CCT images rapidly and with minimal radiation exposure may confer greater benefits, especially in younger patients for whom sedation with general anesthesia is often required for CMR.[20] Cardiac computed tomography also allows for noninvasive coronary assessment, in contrast to cardiac catheterization, which can be performed preoperatively for intracardiac pressure measurements and coronary evaluation, although is not used as a primary diagnostic imaging modality for SVASD.[5]

Accurate diagnosis of the SVASD and associated anomalies is essential for management. Incorrect preoperative diagnosis of IVC-type SVASD was associated with worse technical outcomes, higher rates of reintervention, and longer length of hospital stay.[21] Sinus venosus ASDs are not amenable to percutaneous closure due to their complex anatomy. Surgical repair should be considered in patients with impaired functional capacity or evidence of a hemodynamically significant shunt causing right heart enlargement and a Qp:Qs of greater than 1.5:1.[22] Patients without these signs or symptoms can receive expectant management with regular echocardiographic monitoring. Obtaining baseline and subsequent data on RV size and function as well as defect size is important for monitoring patients who have not undergone surgical repair and assessing for interval chamber size and function improvement in patients whose defects have been repaired. This is ideally performed in a quantitative rather than subjective qualitative manner to minimize the risk of overlooking smaller defects.

The two main methods of surgical SVASD repair are the two-patch technique and the Warden procedure. In the former, the ASD and right atriotomy are each closed with a patch.[23] In the latter, the SVC is divided above the anomalous pulmonary veins and anastomosed to the right atrial appendage, with the residual SVC that receives the anomalous pulmonary venous drainage baffled to the

ASD.[23] Surgical repair generally yields good outcomes, with low rates of morbidity or mortality. A retrospective analysis showed symptomatic improvement in 77% of 115 SVASD patients who underwent surgical repair, with higher preoperative pulmonary artery pressures being strongly associated with reduced symptoms.[24] Postoperative complications such as sinus node dysfunction or stenosis of the pulmonary veins or SVC were uncommon.[24]

In conclusion, SVASD is a rare disorder that can prove challenging to diagnose. Marked otherwise unexplained RV volume overload may be the first clue to the diagnosis of SVASD; TTE, TEE, CCT, CMR, and cardiac catheterization each add incremental value in the workup of SVASD by providing key anatomic and hemodynamic information. Increased awareness of the application of these imaging modalities may help facilitate accurate diagnosis and appropriate management for patients with SVASD.

SUPPLEMENTARY DATA

Supplementary data to this article can be found online at https://doi.org/10.1016/j.case.2021.12.002.

REFERENCES

1. Puri K, Allen HD, Qureshi AM. Congenital heart disease. Pediatr Rev 2017;38:471-86.
2. Williams MR, Perry JC. Arrhythmias and conduction disorders associated with atrial septal defects. J Thorac Dis 2018;10(Suppl 24):S2940-4.
3. Peacock TB. On Malformations of the Human Heart. London: John Churchill; 1858.
4. Ross DN. The sinus venosus type of atrial septal defect. Guys Hosp Rep 1956;105:376-81.
5. Geva T, Martins JD, Walk RM. Atrial septal defects. Lancet 2014;383:1921-32.
6. Lang RM, Bierig M, Devereux RB, Flachskampf FA, Foster E, Pellikka PA, et al. Recommendations for chamber quantification: a report from the American Society of Echocardiography's Guidelines and Standards Committee and the Chamber Quantification Writing Group, developed in conjunction with the European Association of Echocardiography, a branch of the European Society of Cardiology. J Am Soc Echocardiogr 2005;18:1440-63.
7. Saric M, Perk G, Purgess JR, Kronzon I. Imaging atrial septal defects by real-time three-dimensional transesophageal echocardiography: step-by-step approach. J Am Soc Echocardiogr 2010;23:1128-35.
8. Reller MD, McDonald RW, Gerlis LM, Thornburg KL. Cardiac embryology: basic review and clinical correlations. J Am Soc Echocardiogr 1991;4:519-32.
9. Ngai C, Freedberg RS, Latson L, Argilla M, Benenstein RJ, Vainrib AF, et al. Multimodality imaging of scimitar syndrome in adults: a report of four cases. Echocardiography 2018;35:1684-91.
10. Pascoe RD, Oh JK, Warnes CA, Danielson GK, Tajik AJ, Seward JB. Diagnosis of sinus venosus atrial septal defect with transesophageal echocardiography. Circulation 1996;94:1049-55.
11. Shub C, Dimopoulos IN, Seward JB, Callahan JA, Tancredi RG, Schattenberg TT, et al. Sensitivity of two-dimensional echocardiography in the direct visualization of atrial septal defect utilizing the subcostal approach: experience with 154 patients. J Am Coll Cardiol 1983;2:127-35.
12. Marcella CP, Johnson LE. Right parasternal imaging: an underutilized echocardiographic technique. J Am Soc Echocardiogr 1993;6:453-66.
13. Snarr BS, Liu MY, Zuckerberg JC, Falkensammer CB, Nadaraj S, Burnstein D, et al. The parasternal short-axis view improves diagnostic accuracy for inferior sinus venosus type of atrial septal defects by transthoracic echocardiography. J Am Soc Echocardiogr 2017;30:209-15.
14. Narula T, Ali MJ, Lopez FA. A 54-year-old man with shortness of breath and irregular pulse. J La State Med Soc 2010;162:129-33.
15. Puchalski MD, Lui GK, Miller-Hance WC, Burch T, Carron HD, Wong PC, et al. Guidelines for performing a comprehensive transesophageal echocardiographic examination in children and all patients with congenital heart disease: recommendations from the American Society of Echocardiography. J Am Soc Echocardiogr 2019;32:173-215.
16. Kronzon I, Tunick PA, Freedberg RS, Trehan N, Rosenzweig BP, Schwinger ME. Transesophageal echocardiography is superior to transthoracic echocardiography in the diagnosis of sinus venosus atrial septal defect. J Am Coll Cardiol 1991;17:537-42.
17. Badano LP, Boccalini F, Muraru D, Biano LD, Peluso D, Bellu R, et al. Current clinical applications of transthoracic three-dimensional echocardiography. J Cardiovasc Ultrasound 2012;20:1-22.
18. Boxt LM. Magnetic resonance and computed tomographic evaluation of congenital heart disease. J Magn Reson Imaging 2004;19:827-47.
19. Valente AM, Sena L, Powell AJ, Del Nido PJ, Geva T. Cardiac magnetic resonance imaging evaluation of sinus venosus defects: comparison to surgical findings. Pediatr Cardiol 2007;28:51-6.
20. Tretter JT, Chikkabyrappa S, Spicer DE, Backer CL, Mosca RS, Anderson RH, et al. Understanding the spectrum of sinus venosus interatrial communications. Cardiol Young 2017;27:418-26.
21. Banka P, Bacha E, Powell AJ, Benavidez OJ, Geva T. Outcomes of inferior sinus venosus defect repair. J Thorac Cardiovasc Surg 2011;142:517-22.
22. Stout KK, Daniels CJ, Aboulhosn JA, Bozkurt B, Broberg CS, Colman JK, et al. 2018 AHA/ACC guideline for the management of adults with congenital heart disease: executive summary: a report of the American College of Cardiology/American Heart Association task force on clinical practice guidelines. Circulation 2019;130:e637-97.
23. Liava'a M, Kalfa D. Surgical closure of atrial septal defects. J Thorac Dis 2018;10(Suppl 24):S2931-9.
24. Attenhofer Jost CH, Connolly HM, Danielson GK, Bailey KR, Schaff HV, Shen WK, et al. Sinus venosus atrial septal defect: long-term postoperative outcome for 115 patients. Circulation 2005;112:1953-8.